2017 SCEC Report

Microseismicity, geodetic coupling, and earthquake variability on heterogeneous faults: A case study of the Anza section of the San Jacinto Fault

PI: Yuri Fialko

Institution: Institute of Geophysics and Planetary Physics, Scripps Institution of Oceanography, University of California, San Diego

Proposal Category: B. Integration and Theory

Priority objectives addressed by the proposed research:

P1.d. Quantify stress heterogeneity on faults at different spatial scales, correlate the stress concentrations with asperities and geometric complexities, and model their influence on rupture initiation, propagation, and arrest.

P3.b. Constrain the active geometry and rheology of the ductile roots of fault zones.

P5.a. Develop earthquake simulators that encode the current understanding of earthquake predictability.

Focus Group: FARM, SDOT

Dates: Feb. 1, 2017 – Jan. 31, 2018

1 Summary

The main goal of this study is to develop three-dimensional (3D) models of faults governed by laboratory-based friction laws for the Anza section of the San Jacinto fault (SJF) and to improve our understanding of the seismic behavior of SJF and regional seismic hazard associated with major events. Unlike the nearby largely quiescent San Andreas fault, the SJF is the most seismically active fault in Southern California. Microseismicity (M 2–4) near Anza predominantly occurs at depths of 10–18 km, whereas larger events (M∼5) occasionally occur near the bottom of the seismogenic zone. Despite these microseismic activity, the Anza section is the only part of the SJF that has not ruptured in major (M 6–7) earthquakes over the past 200 years, hence considered a "seismic gap" [*Thatcher et al.*, 1975; *Sanders and Kanamori*, 1984] that poses seismic risks to nearby populated areas. The diverse microseismic activity around the seismic gap, along with geodetic observations of interseismic strain accumulation [*Lindsey et al.*, 2013] and historical and paleoseismic records of past events [*Rockwell et al.*, 2006] constitutes a rich dataset for a major seismogenic fault. Through a case study of the SJF that involves developing numerical models in accordance with geophysical observations, we aim to understand the conditions of and interactions between seismic gap and nearby seismically active regions and explore plausible large earthquake scenarios on such faults.

In our earlier work, funded by SCEC in 2016–2017, we developed a 3D model of fault with spatially variable rate-and-state frictional properties that can reproduce the relation between seismicity and geodetic locking depths relevant to the Anza section [*Jiang and Fialko*, 2016]. The study was motivated by the finding of a discrepancy between the anomalously shallow locking depth inferred from geodetic measurements (10.4±1.3km) [*Lindsey et al.*, 2013] and much larger maximum depths of seismicity (14–18 km) near Anza, which is at odds with empirical and theoretical studies [*Smith-Konter et al.*, 2011; *Jiang and Lapusta*, 2017]. We suggest that the observations can be explained by abundant aseismic transient processes, as a result of highly heterogeneous frictional properties at the base of the seismogenic zone. Our model also predicts that large earthquakes on the fault can penetrate beyond the geodetic locking depth and to the maximum depth of microseismicity. However, due to our focus on the overall depth relation, the model has along-strike near-uniform conditions and cannot be directly used to understand more detailed observations, such as the juxtaposition of Anza seismicity gap and neighboring seismically active regions.

Over the last year, we have further developed models of faults with along-strike variations in frictional properties that are more closely tailored to the case of Anza. We incorporate enhanced dynamic weakening (DW) that is documented at high-slip-rate experiments, in addition to the low-slip-rate rate-and-state friction laws that were only considered in the earlier study. Our focus is on constraining fault frictional properties of the Anza seismicity gap and surrounding areas and the interactions of seismic and aseismic slip in these areas. Our main findings are as follows:

- Along-strike variations in fault frictional properties lead to complex earthquake slip patterns. The Anza seismicity gap can be explained by a larger fault area that is more susceptible to DW during earthquake rupture and has lower interseismic stresses, compared to nearby areas. The lower-stressed region, along with variable seismogenic zone width, contributes to a complex earthquake slip history characterized by partial ruptures of different sizes and system-sized events every hundreds of years, largely consistent with paleoseismic studies at Anza.

- Large-scale geodetic observations constrain the over behavior of faulting, while pronounced smaller-scale variations can still exist. Local deeper penetration of large earthquakes can be reconciled with a shallower regional geodetic locking depth if nearby areas host aseismic transients.

- Interactions of seismic and aseismic slip is highly dependent on the heterogenous state of fault frictional properties. In 2D models with stochastic distribution of frictional properties, a higher

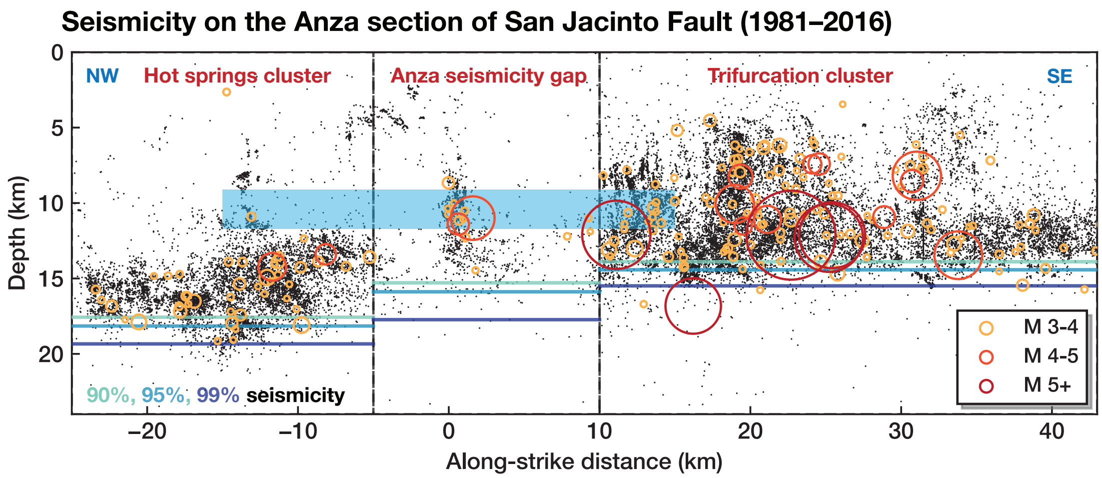

Figure 1: Seismicity along the San Jacinto Fault (SJF) in Southern California (1981–2011) [*Hauksson et al.*, 2012]. Hypocenter locations of $M_w < 3$ earthquakes are denoted by black dots. The approximate sizes of $M_w \geq 3$ earthquakes are shown as circles based on a circular crack model [*Eshelby*, 1957] with the same seismic moment and 3 MPa stress drop. Horizontal lines denote depths above which the specified percentage of earthquakes has occurred over the segment. Blue band indicates the 1σ uncertainty range for the geodetic locking depth [*Lindsey et al.*, 2013].

moment release through seismic slip is promoted by a larger amplitude in heterogeneity, a larger maximum wavelength, and a faster average loading rate.

2 Reproducing observations from the Anza section in models with laterally variable fault properties

The seismicity patterns observed on the Anza section of the SJF is highly variable along the strike (Fig. 1) [*Sanders*, 1990; *Hauksson et al.*, 2012]. For seismically active segments, the general trend of deepening of seismicity from southeast (SE) to northwest (NW) can be explained in terms of a regional decrease in the geothermal gradient [*Doser and Kanamori*, 1986]. The Anza seismicity gap is seismically inactive over much of the seismogenic zone, similar to the seismic quiescence that is typical for the Cholame, Carrizo, Mojave, and Coachella segments of the Southern San Andreas Fault. *Jiang and Lapusta* [2016] suggested that the seismic quiescence of these major segments may be explained by the penetration of earthquake ruptures into the deeper creeping fault extensions, likely aided by enhanced dynamic weakening (DW) as documented in high-velocity laboratory friction experiments [*Di Toro et al.*, 2011]. Such deeper ruptures effectively suppress the nucleation of microseismicity at the bottom of the seismogenic zone in most of the interseismic period. Similarly, fault areas at the Anza seismicity gap may also be more susceptible to DW, leading to a deeper rupture, and hence a greater geodetic locking depth compared to nearby segments.

We have developed 3D models with along-strike variations in fault frictional properties to reproduce and understand multiple geophysical observations (Fig. 2a). The model features an increasing width of the seismogenic zone as suggested by the regional geotherm. The shallow seismogenic zone has velocity-weakening (VS) frictional properties, hence prone to earthquake nucleation. The bottom of the seismogenic zone has velocity-neutral (VN) properties (still VW but have much larger nucleation sizes due to small $(a - b)$ values). The surrounding areas have velocity-strengthening (VS) frictional properties that tend to creep stably. At high slip rates, we assume that all VW regions are susceptible to DW and so is the VN area in the middle fault section, which correspond to the Anza seismicity gap.

Complexity in earthquake slip naturally arises in these models. Major (M5.5–6.5) earthquakes occasionally rupture a fraction of the seismogenic zone, whereas less frequent but larger earthquakes span the entire fault (Fig. 2b–c). The width of the seismogenic zone affect the size and frequency of the smaller events due to different average stressing rates, leading to more events on the sections to the right than the left (Fig. 2d). The entire middle section only participates in earthquake rupture during system-sized events, and serves as an earthquake barrier to smaller events. The coexistence of partial and system-sized earthquakes with a recurrence period of 200–300 yr and variability in earthquake slip at the surface are largely consistent with paleoseismic studies on this fault section [*Rockwell et al.*, 2006; *Salisbury et al.*, 2012].

Since VN regions are ineffective in stopping earthquake ruptures, coseismic slip tapers down to the downdip edge of the seismogenic zone, in either partial or system-sized events. Due to the imposed deeper DW, larger coseismic slip occurs in the VN area of the middle section, which we refer to as local deeper rupture. Presumably, pronounced, deeper seismic slip would correspond to a larger geodetic locking depth [*Jiang and Lapusta*, 2017]. We focus on the conditions on the fault during a typical interseismic period (Fig. 3). More reduced interseismic slip rates on the fault indeed result from the deeper coseismic rupture at the middle section, indicating lower shear stresses and stressing rates (Fig. 3a–b). When we consider only the depth-profile along vertical cross-sections and use them to estimate the local effective geodetic locking depth in a 2D problem, we find that indeed the middle section has a deeper locking depth than what would be if deeper DW is absent. As expected, the section to the right has a shallower locking depth, due to a smaller width of the seismogenic zone and occurrence of some aseismic transients. The overall geodetic locking depth is somewhere between these estimates, indicating that local deeper rupture in the Anza seismicity gap may still be reconciled with a regional shallow geodetic locking depth, if there are indeed aseismic transients as suggested by some recent studies [e.g., *Inbal et al.*, 2017].

These results suggest that more detailed inferences from geodetic observations are needed to validate and refine these models. At the moment, we are motivated to further test whether we can resolve along-strike variations in the locking depths over the Anza section from InSAR data using different lines-of-sight, as well as continuous and campaign GPS data. Presence (or absence) of systematic along-strike variations in the fault locking depth will provide critical constraints for our models.

3 Partitioning of seismic and aseismic slip on faults with spatially heterogeneous frictional properties

The VN transition zones in our 3D models are designed to promote frequent aseismic transients and they inevitably accommodate some coseismic slip due to small strength excess. In models with uniform VN frictional properties, we found that the parameter space for a and b that lead to pronounced aseismic transients is rather narrow. We then focus on 2D smaller-scale models for such a transition zone to better understand the controlling factors for the interaction between seismic and aseismic slip. The computationally efficient 2D models allow us to explore an ensemble of models with heterogeneous frictional properties that follow a stochastic distribution.

In these 2D models, we assume a fractal-like (self-similar) distribution of $(a-b)$ values relative to a background level corresponding to a uniform model (Fig. 4a). We simulate seismic and aseismic slip in such models, as defined by a threshold slip rate value of 0.1 m/s. Seismicity often occurs in persistent “asperities” where local nucleation size is small enough, and aseismic

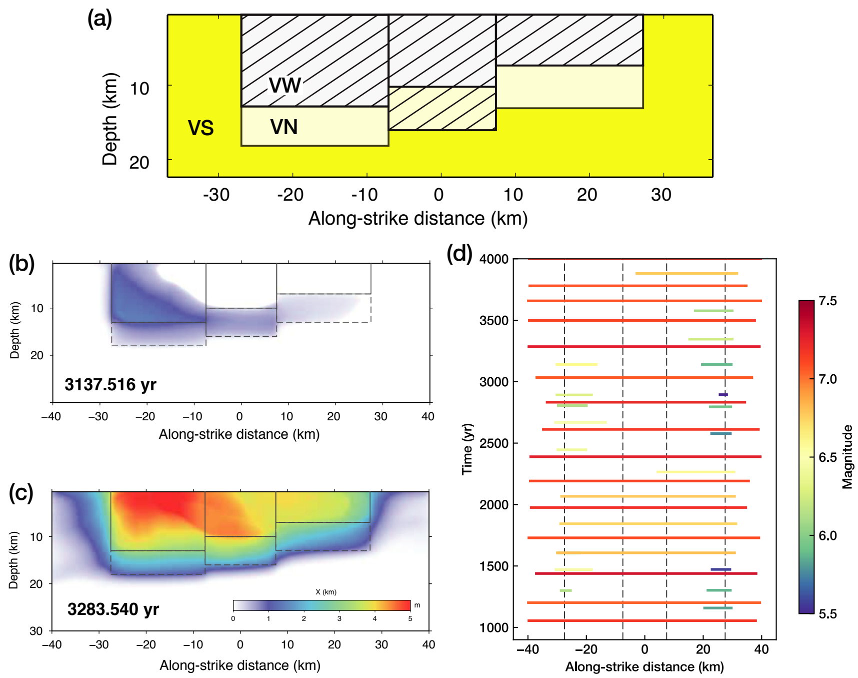

Figure 2: Earthquake history in a 3D model of a heterogeneous fault. (a) Model setup. The depth limit of velocity-weakening (VW) fault areas (in gray) increases along the strike, surrounded by velocity-strengthening (VS) fault areas. The transition zone between the VW and VS areas are referred to as the velocity-neutral (VN) areas, where seismic and aseismic slip overlap. The dashed areas indicate where enhanced dynamic weakening (DW) is active. (b) Partial and (c) system-sized earthquake ruptures in the simulation, with coseismic slip in color. (d) The time of earthquakes and rupture length of these events at the surface. The event magnitude is colored. Dashed lines mark the boundary between the three fault segments.

creep occurs between these “asperities” and relax and transfer stress to nearby areas (Fig. 4b). Both processes can contribute to a sizable fraction of the total moment release in the fault model. We identify several parameters with a strong influence on the fraction of seismic moment release on such fault areas: (1) the amplitude of heterogeneity; (2) the maximum cut-off wavelength; and (3) the long-term loading rate. In general, a higher proportion of moment would be released seismically on a heterogeneous fault with a larger variation and a longer-wavelength component in the distribution of $(a - b)$ values, and a faster loading rate.

We plan to use the insights gained in these 2D models to guide the development of fault models that produce large earthquakes as well as seismicity and slow slip events. The established relations between heterogeneous frictional field and fault behavior will also aid other future studies, e.g., generating and studying synthetic earthquake catalogues.

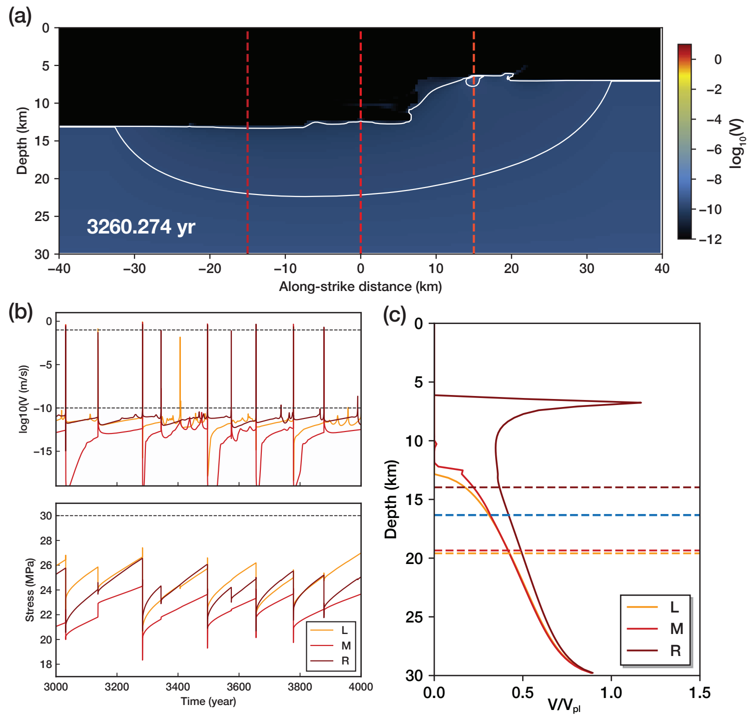

Figure 3: Along-strike variation in the behavior of a 3D fault model. (a) Spatial distribution of interseismic slip rates on the fault (in the year 3260). Dashed lines are cross-sections through different fault areas (the left, middle, and right marked as L, M, and R, respectively). (b) The long-term evolution of (top) slip rates and (bottom) shear stresses in different fault areas. (c) Depth profiles of slip rates (normalized by the plate loading rate V_{pl}) along the cross-sections marked in (a). The horizontal dashed lines with corresponding colors indicate the inferred effective geodetic locking depth in a 2D problem; the blue dash line indicate an estimate of geodetic locking depth from the 2D surface velocity field due to the fault slip rate distribution shown in (a).

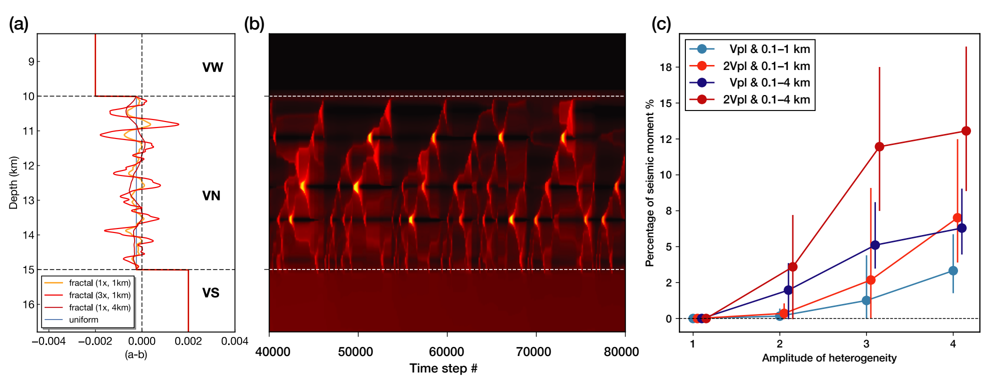

Figure 4: Seismic and aseismic slip in 2D heterogeneous models. (a) the transition VN zone between the VW and VS areas. The lines indicate cases with different distributions of frictional properties in terms of $a-b$. The cases with heterogeneous frictional properties feature fractal distributions of $(a-b)$, which are generated with assumed amplitudes and wavelength ranges. The amplitude is represented by the standard deviation of the fractal distribution, relative to the absolute $(a-b)$ value for the case with uniform properties. (b) Evolution of the depth-dependent fault slip rates (colored on the logarithmic scale). Note that time step, rather than time, is used to highlight the seismic events. (c) The percentage of seismic to total moment release for different cases. Two plate loading rates (10^{-9} and $2 \cdot 10^{-9}$ m/s) and two wavelength ranges (0.1–1 and 0.1–4 km) are considered.

References

Di Toro, G., R. Han, T. Hirose, N. De Paola, S. Nielsen, K. Mizoguchi, F. Ferri, M. Cocco, and T. Shimamoto, Fault lubrication during earthquakes, *Nature*, *471*(7339), 494–498, doi:10.1038/nature09838, 2011.

Doser, D. I., and H. Kanamori, Depth of seismicity in the Imperial Valley region (1977-1983) and its relationship to heat flow, crustal structure, and the October 15, 1979, earthquake, *J. Geophys. Res.*, *91*, 675–688, 1986.

Eshelby, J. D., The determination of the elastic field of an ellipsoidal inclusion, and related problems, *Proceedings of the Royal Society of London A: Mathematical, Physical and Engineering Sciences*, *241*(1226), 376–396, doi:10.1098/rspa.1957.0133, 1957.

Hauksson, E., W. Yang, and P. M. Shearer, Waveform relocated earthquake catalog for Southern California (1981 to June 2011), *Bull. Seismol. Soc. Am.*, *102*(5), 2239–2244, doi:10.1785/0120120010, 2012.

Inbal, A., J. Ampuero, and J. Avouac, Locally and remotely triggered aseismic slip on the central san jacinto fault near anza, ca, from joint inversion of seismicity and strainmeter data, *Journal of Geophysical Research: Solid Earth*, *122*(4), 3033–3061, doi:10.1002/2016JB013499, 2017.

Jiang, J., and Y. Fialko, Reconciling seismicity and geodetic locking depths on the Anza section of the San Jacinto fault, *Geophysical Research Letters*, pp. n/a–n/a, doi:10.1002/2016GL071113, 2016GL071113, 2016.

Jiang, J., and N. Lapusta, Deeper penetration of large earthquakes on seismically quiescent faults, *Science*, *352*(6291), 1293–1297, doi:10.1126/science.aaf1496, 2016.

Jiang, J., and N. Lapusta, Connecting depth limits of interseismic locking, microseismicity, and large earthquakes in models of longterm fault slip, *Journal of Geophysical Research: Solid Earth*, *122*(8), 6491–6523, doi:10.1002/2017JB014030, 2017.

Lindsey, E. O., V. J. Sahakian, Y. Fialko, Y. Bock, S. Barbot, and T. K. Rockwell, Interseismic strain localization in the San Jacinto Fault Zone, *Pure. Appl. Geophys.*, doi:10.1007/s00024-013-0753-z, 2013.

Rockwell, T., G. Seitz, T. Dawson, and J. Young, The long record of San Jacinto fault paleoearthquakes at Hog Lake: Implications for regional patterns of strain release in the southern San Andreas fault system, *Seismol. Res. Lett*, *77*(2), 270, 2006.

Salisbury, J. B., T. K. Rockwell, T. J. Middleton, and K. W. Hudnut, LiDAR and field observations of slip distribution for the most recent surface ruptures along the Central San Jacinto Fault, *Bulletin of the Seismological Society of America*, *102*(2), 598–619, doi:10.1785/0120110068, 2012.

Sanders, C. O., Earthquake depths and the relation to strain accumulation and stress near strike-slip faults in southern California, *J. Geophys. Res.*, *95*(B4), 4751–4762, doi:10.1029/JB095iB04p04751, 1990.

Sanders, C. O., and H. Kanamori, A seismotectonic analysis of the Anza Seismic Gap, San Jacinto Fault Zone, southern California, *J. Geophys. Res.*, *89*(B7), 5873–5890, doi:10.1029/JB089iB07p05873, 1984.

Smith-Konter, B. R., D. T. Sandwell, and P. M. Shearer, Locking depths estimated from geodesy and seismology along the San Andreas Fault System: Implications for seismic moment release, *J. Geophys. Res.*, *116*(B6), B06,401, doi:10.1029/2010JB008117, 2011.

Thatcher, W., J. A. Hileman, and T. C. Hanks, Seismic slip distribution along the San Jacinto fault zone, Southern California, and its implications, *Geological Society of America Bulletin*, *86*(8), 1140–1146, doi:10.1130/0016-7606(1975)86¡1140:SSDATS¿2.0.CO;2, 1975.